Cubic-quartic bright optical solitons with improved Adomian decomposition method

O. González-Gaxiola [a], Anjan Biswas [b,c,d,e], Fouad Mallawi [c], Milivoj R. Belic [f]

[a] Departamento de Matemáticas Aplicadas y Sistemas, Universidad Autónoma Metropolitana-Cuajimalpa, Vasco de Quiroga 4871, 05348 Mexico City, Mexico
[b] Department of Physics, Chemistry and Mathematics, Alabama A&M University, Normal, AL 35762-7500, USA
[c] Department of Mathematics, King Abdulaziz University, Jeddah-21589, Saudi Arabia
[d] Department of Applied Mathematics, National Research Nuclear University, 31 Kashirskoe Shosse, Moscow-115409, Russian Federation
[e] Department of Mathematics and Statistics, Tshwane University of Technology, Pretoria-0008, South Africa
[f] Science Program, Texas A&M University at Qatar, Doha, Qatar

HIGHLIGHTS

- Optical soliton solutions for the perturbed nonlinear Schrodinger's equation are revealed.
- Quadratic-cubic nonlinearity is considered.
- Bright optical solitons are retrieved by the help of the IADM.
- The numerical results together with high level accuracy plots are exhibited.
- The method proposed herein works with high degree of accuracy.

GRAPHICAL ABSTRACT

Cubic-quartic soliton transmission having power law of nonlinearity refractive index.
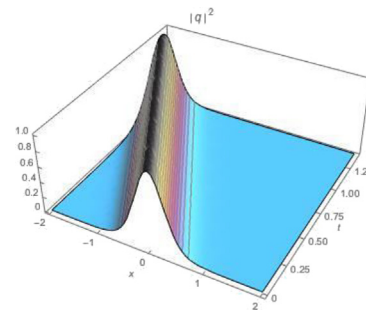
ARTICLE INFO

ABSTRACT

This paper numerically retrieves cubic-quartic solitons having power law of nonlinearity refractive index. An improvement of the Adomian decomposition scheme is the adopted algorithm of this work. The results are displayed along with the established error analysis.

© 2019 The Authors. Published by Elsevier B.V. on behalf of Cairo University. This is an open access article under the CC BY-NC-ND license (http://creativecommons.org/licenses/by-nc-nd/4.0/).

Introduction

One of the emerging concepts from mathematical photonics is "cubic-quartic (CQ) solitons" [1–7,9,10]. This appears when group velocity dispersion (GVD) runs low and hence discarded. This

was first introduced a couple of years ago as a follow-up to the concept of "quartic solitons" which was a prequel paper to the first paper on CQ solitons [8]. It is noted that quartic solitons cannot be analytically studied and therefore one must remain contended with numerical solutions only. In order to understand the behavior of solitons in absence of GVD the concept of CQ solitons was subsequently introduced. Later spectrums of results have started pouring in with CQ solitons.

While all of the works thus far on CQ solitons are analytical in character, it now time to take a fresher look at such solitons from a numerical perspective. The current paper thus addresses CQ solitons from a numerical standpoint. The algorithm that displays the results is an improved version of Adomian decomposition method (IADM) scheme. The focus is on power law nonlinearity refractive index. The details of the scheme are inked and the results are displayed in the upcoming sections.

The model

The cubic-quartic (CQ) NLSE including third and fourth order dispersion but without GVD is given by [1]:

$$iq_t + iaq_{xxx} + bq_{xxxx} + c|q|^{2m}q = 0, \quad m \in \mathbb{N}. \tag{1}$$

Here, in Eq. (1), $q(x,t)$ the complex-valued wave amplitude that governs the evolution of a nonlinear wave, x is a longitudinal variable and t is a co-moving time and $i = \sqrt{-1}$. Besides a and b respectively represent coefficients of third and fourth order dispersions. Finally c is the coefficient of power law of refractive index where m stands for the power law factor.

Exact analytical bright and singular soliton solutions for the CQ model (1) were recently obtained in [1] with the help the of the undetermined coefficients method and before in [8] pure-quartic solitons propagation was studied.

Cubic-quartic bright optical solitons

The bright CQ 1-soliton solution to (1) was found by the authors in [1] and is given by

$$q(x,t) = A\mathrm{sech}^{\frac{2}{m}}[B(x - vt)]e^{i[-\kappa x + \omega t + \theta_0]}. \tag{2}$$

In Eq. (2), v is the soliton velocity, ω is the angular velocity, κ is the soliton frequency, and θ_0 is the phase center.

The amplitude A and the inverse width B of the CQ 1-soliton are given by

$$A = \left[-\frac{(m+2)(3m+2)P_2^2}{2bc(m^2+2m+2)^2}\right]^{\frac{1}{2m}}, \quad B$$

$$= \frac{m}{2}\left[-\frac{P_2}{b(m^2+2m+2)}\right]^{\frac{1}{2}}, \tag{3}$$

where $P_2 = \frac{3a^2}{8b}$.

The velocity v and the angular velocity ω of the CQ 1-soliton are given by

$$v = -3a\kappa^2 + 4b\kappa^3, \quad \omega$$

$$= \frac{b\kappa^3(b\kappa - a)(m^2+2m+2)^2 - 9\kappa^2(m+1)^2(a - 2b\kappa)^2}{b(m^2+2m+2)^2}, \tag{4}$$

where the soliton frequency κ, is related to the coefficients of the model by $\kappa = \frac{a}{4b}$.

Material and methods

A modification of the standard Adomian decomposition method (ADM) was proposed by A. M. Wazwaz first in [11] and shortly after the modification was improved in [12] by A. M. Wazwaz and S. M. El-Sayed. This improvement to the Adomian decomposition method was established based on the assumption that the initial condition can be decomposed into a series of functions in the spatial variable. We will use the IADM to solve the Eq. (1) in the case of bright solitons through several examples.

Supposing that $q(x,t) = u_1(x,t) + iu_2(x,t)$, Eq. (1) can be split into real and imaginary parts

$$-L_t u_2 - aR_3 u_2 + bR_4 u_1 + cN_1(u_1, u_2) = 0$$

$$L_t u_1 + aR_3 u_1 + bR_4 u_2 + cN_2(u_1, u_2) = 0, \tag{6}$$

where $L_t = \frac{\partial}{\partial t}$ and $L_t^{-1} = \int_0^t(\cdot)ds$. Each R_j is a linear differential operator, that is, $R_j = \frac{\partial^j}{\partial x^j}$, $j = 3, 4$ and the nonlinear terms N_1 and N_2 are given for the cases $m = 1$ and $m = 2$ respectively, by

$$\begin{cases} N_1(u_1, u_2) = u_1^2 + u_1 u_2^2 \\ N_2(u_1, u_2) = u_2^3 + 2u_1^2 u_2 - u_1 u_2, \end{cases} \tag{7}$$

$$\begin{cases} N_1(u_1, u_2) = u_1^5 + 2u_1^3 u_2^2 + u_1 u_2^4 \\ N_2(u_1, u_2) = u_2^5 + 2u_1^2 u_2^3 + u_1^4 u_2. \end{cases} \tag{8}$$

As the operator L_t is invertible, applying the operator L_t^{-1} to both sides of Eqs. (5) and (6), we get

$$u_1(x,t) = \Re e(q(x,0)) - L_t^{-1}(aR_3 u_1 + bR_4 u_2 + cN_2(u_1, u_2)) \tag{9}$$

$$u_2(x,t) = \Im m(q(x,0)) + L_t^{-1}(-aR_3 u_2 + bR_4 u_1 + cN_1(u_1, u_2)), \tag{10}$$

where $u_{1,0}(x,0) = \Re e(q(x,0))$ and $u_{2,0}(x,0) = \Im m(q(x,0))$.

Assume that Eq. (1) has the following series solution [13]:

$$q(x,t) = u_1(x,t) + iu_2(x,t) = \sum_{n=0}^{\infty} u_{1,n}(x,t) + i\sum_{n=0}^{\infty} u_{2,n}(x,t)., \tag{11}$$

The components $u_{j,n}$ for $j = 1, 2$ will be determined recurrently. Also the nonlinear operators N_1 and N_2 are decomposed as follows:

$$N_j(u_1, u_2) = \sum_{n=0}^{\infty} A_{j,n}(u_{j,0}, u_{j,1}, \ldots, u_{j,n}), \quad j = 1, 2 \tag{12}$$

where $\{A_{j,n}\}_{n=0}^{\infty}$ is the so-called Adomian polynomials sequence. A novel method to calculate the Adomian polynomials was recently proposed in [14], namely

$$A_{j,0}(u_{j,0}) = N_j(u_{j,0}) \tag{13}$$

$$A_{j,n}(u_{j,0}, u_{j,1}, \ldots, u_{j,n}) = \frac{1}{2\pi}\int_{-\pi}^{\pi} N_j\left(\sum_{k=0}^{n} u_{j,k}e^{ik\omega}\right)e^{-in\omega}d\omega, \quad n \geqslant 1. \tag{14}$$

As we can see, in this algorithm tedious calculations of high derivatives are not required.

Hence from Eqs. (9), (10) (11) and (12), we have the following iterative algorithm to compute the solution components:

$$u_1(x,t) = \sum_{n=0}^{\infty} f_n(x)$$

$$- L_t^{-1}\left(aR_3\left(\sum_{n=0}^{\infty} u_{1,n}(x,t)\right) + bR_4\left(\sum_{n=0}^{\infty} u_{2,n}(x,t)\right) + c\sum_{n=0}^{\infty} A_{2,n}\right), \tag{15}$$

$$u_2(x,t) = \sum_{n=0}^{\infty} g_n(x)$$

$$+ L_t^{-1}\left(-aR_3\left(\sum_{n=0}^{\infty} u_{2,n}(x,t)\right) + bR_4\left(\sum_{n=0}^{\infty} u_{1,n}(x,t)\right) + c\sum_{n=0}^{\infty} A_{1,n}\right), \tag{16}$$

According to IADM, we are assuming that the initial conditions will be decomposed in series, namely:

Table 1
The absolute error when t = 0.1, t = 0.2, t = 0.3 and t = 0.5 for case m = 1 and subcase (i).

x	Error when t = 0.1	Error when t = 0.2	Error when t = 0.3	Error when t = 0.5
−1.00	1.7×10^{-9}	3.7×10^{-9}	3.1×10^{-8}	6.4×10^{-8}
−0.50	3.1×10^{-8}	6.8×10^{-8}	4.5×10^{-7}	5.1×10^{-7}
0.00	2.0×10^{-8}	5.5×10^{-7}	2.1×10^{-7}	6.6×10^{-8}
0.50	2.6×10^{-9}	1.4×10^{-8}	6.1×10^{-8}	8.1×10^{-8}
1.00	4.4×10^{-10}	7.1×10^{-9}	2.3×10^{-8}	5.5×10^{-8}
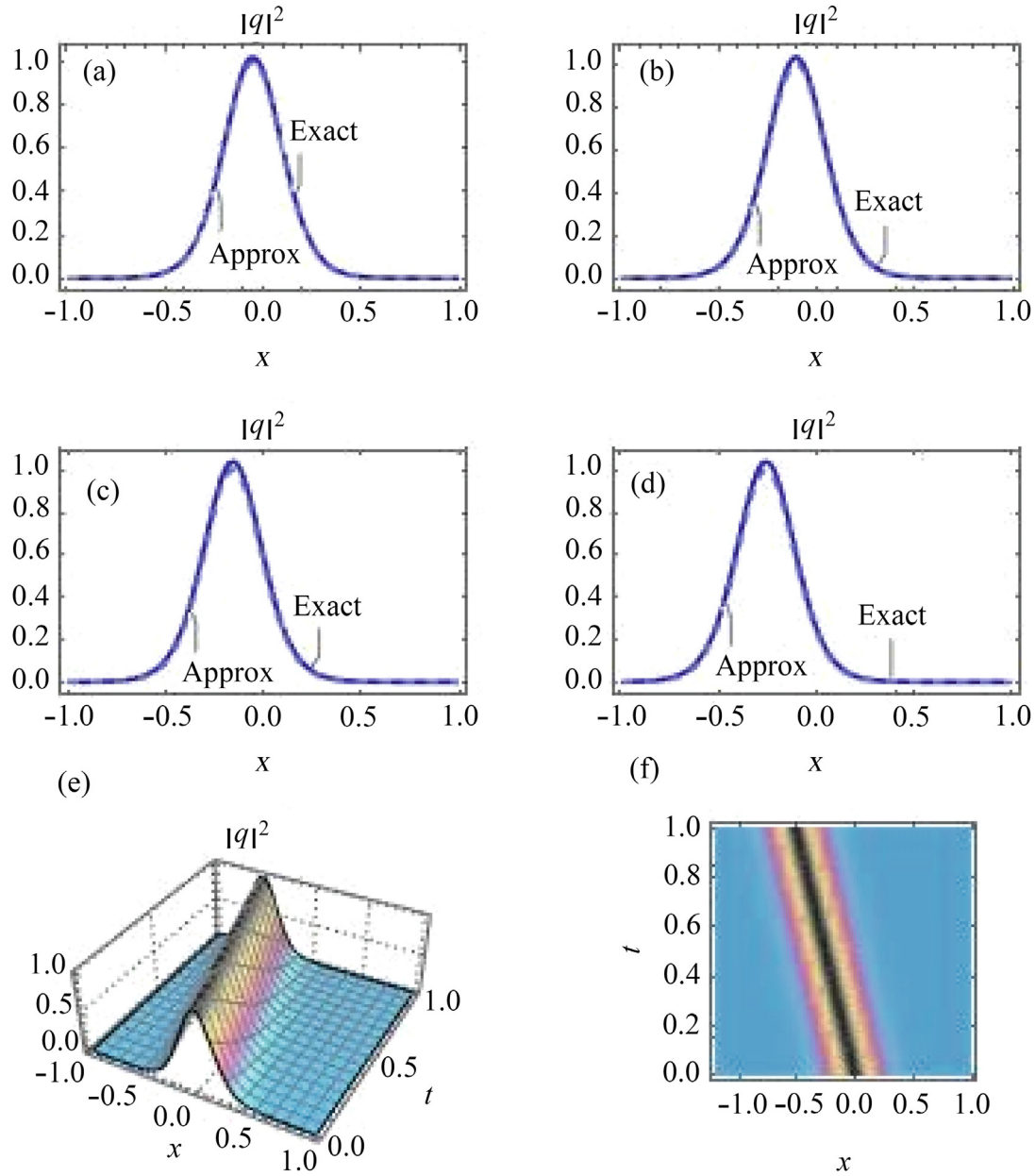
Fig. 1. Comparison of proposed method solution by IADM and exact solution for $-1 < x < 1$ and (a) t = 0.1, (b) t = 0.2, (c) t = 0.3, (d) t = 0.5. (e) Profile of the solution q(x,t) and (f) density plot of the solution. Case m = 1 and subcase (i) with N = 15.

$$\Re e(q(x,0))) = \sum_{n=0}^{\infty} f_n(x), \quad \Im m(q(x,0)) = \sum_{n=0}^{\infty} g_n(x). \quad (17)$$

Now we proceed to approximate solution components $u_{1,n}(x,t)$ and $u_{2,n}(x,t)$ for $n \geqslant 0$ using IADM by the following recursive relationships:

$$\begin{cases} u_{1,0}(x,t) = f_0(x), \\ u_{1,k+1}(x,t) = f_{k+1}(x) - \int_0^t (aR_3(u_{1,k}(x,\zeta) \\ +bR_4(u_{2,k}(x,\zeta)) + cA_{2,k})d\zeta, \ k \geqslant 0. \end{cases} \quad (18)$$

Table 2
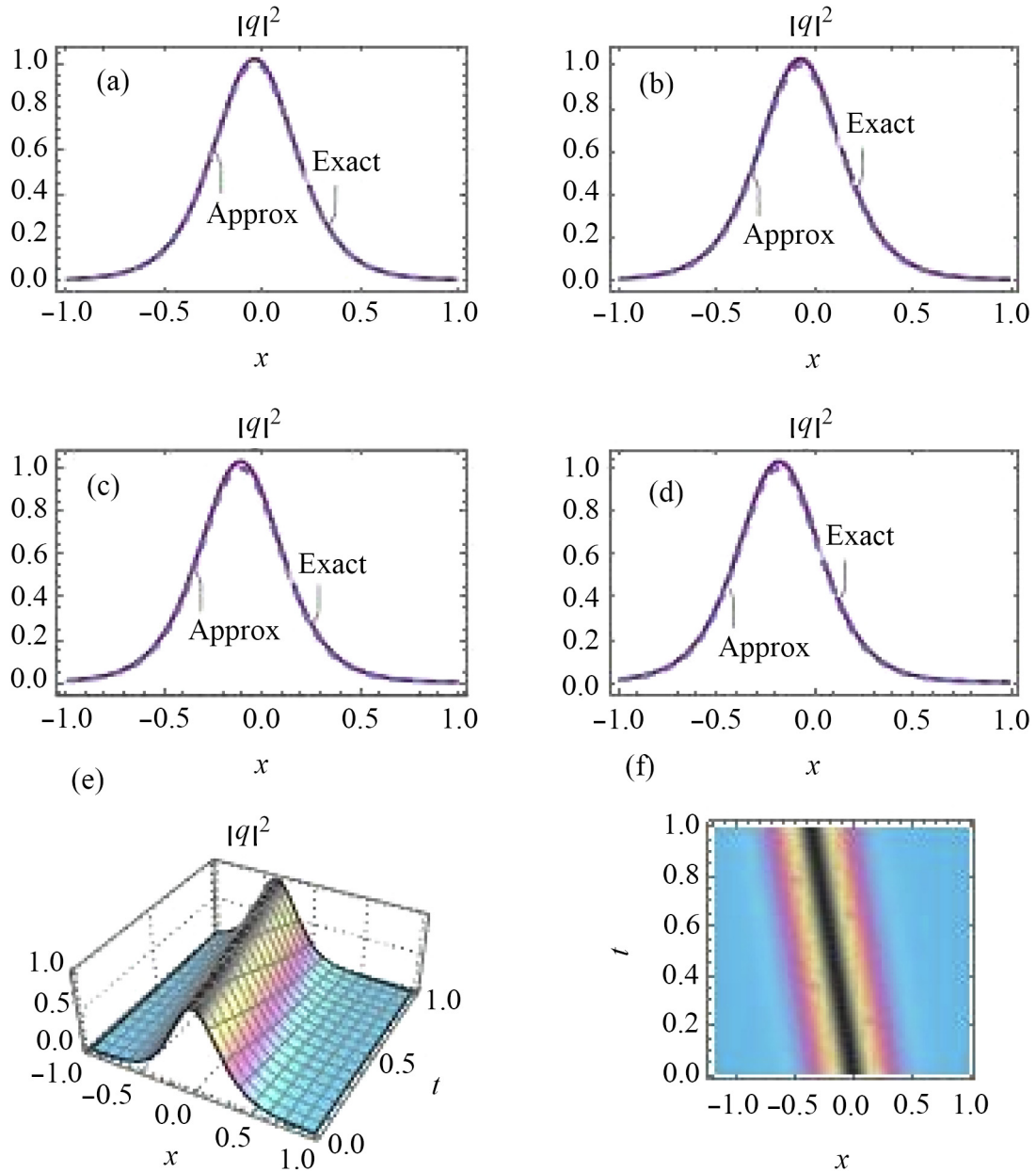The absolute error when t = 0.1, t = 0.2, t = 0.3 and t = 0.5 for case m = 1 and subcase (ii).

x	Error when t = 0.1	Error when t = 0.2	Error when t = 0.3	Error when t = 0.5
−1.50	1.9×10^{-10}	3.5×10^{-10}	4.0×10^{-9}	5.2×10^{-8}
−1.00	2.1×10^{-10}	3.7×10^{-10}	4.8×10^{-9}	7.4×10^{-7}
−0.50	2.6×10^{-9}	1.8×10^{-8}	3.3×10^{-8}	2.5×10^{-6}
0.00	2.8×10^{-8}	2.0×10^{-9}	5.6×10^{-8}	5.0×10^{-7}
0.50	1.8×10^{-9}	2.4×10^{-9}	4.1×10^{-9}	2.3×10^{-7}
1.00	2.2×10^{-9}	3.0×10^{-10}	3.7×10^{-9}	2.0×10^{-8}
1.50	1.4×10^{-10}	2.2×10^{-10}	1.1×10^{-10}	4.1×10^{-9}
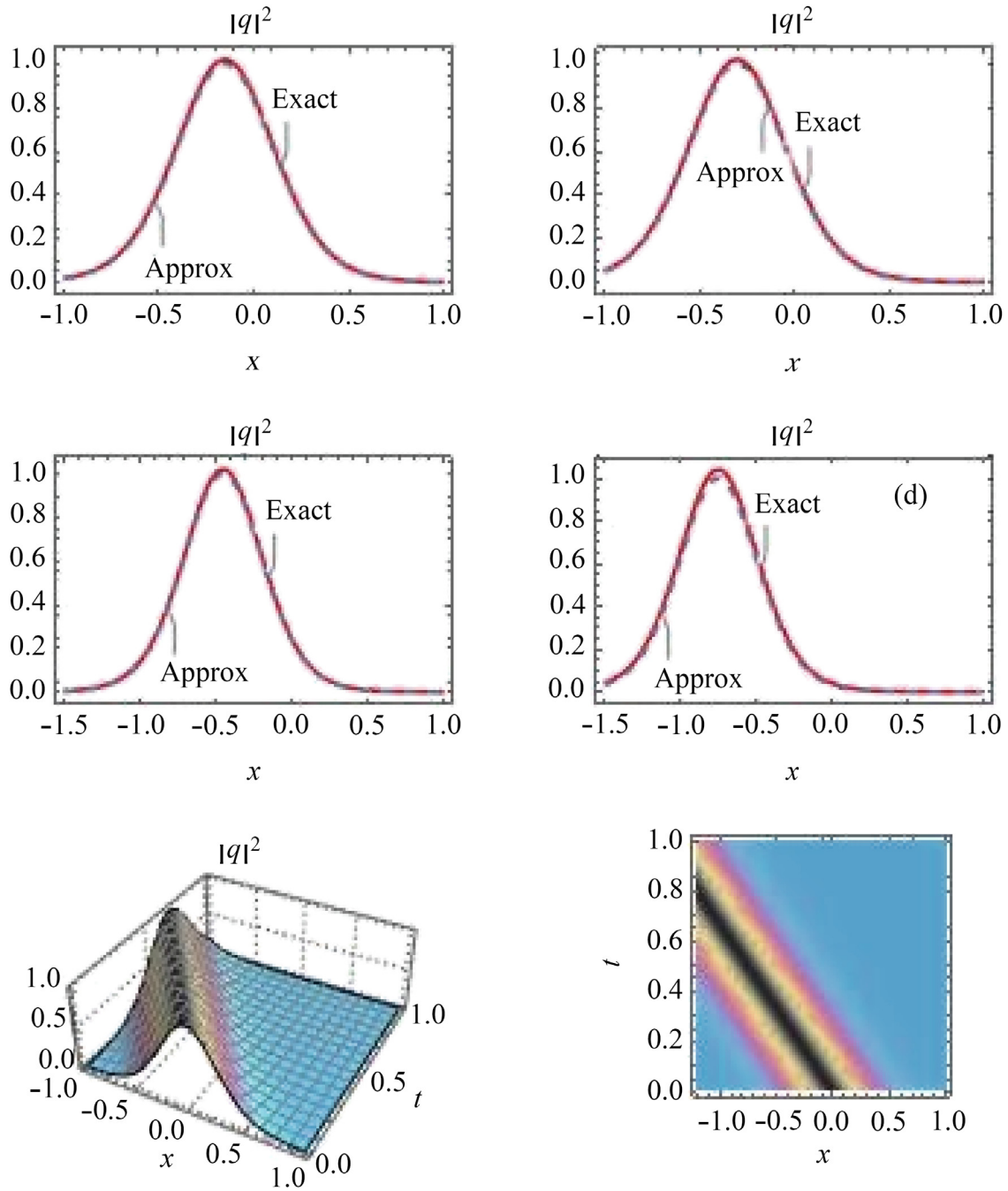
Fig. 2. Comparison of proposed method solution by IADM and exact solution for −1.5 < x < 1.5 and (a) t = 0.1, (b) t = 0.2, (c) t = 0.3, (d) t = 0.5. (e) Profile of the solution q(x,t) and (f) density plot of the solution. Case m = 1 and subcase (ii) with N = 15.

Table 3
The absolute error when t = 0.1, t = 0.2, t = 0.3 and t = 0.5 for case m = 2 and subcase (iii).

x	Error when t = 0.1	Error when t = 0.2	Error when t = 0.3	Error when t = 0.5
−1.00	2.0×10^{-10}	1.7×10^{-9}	6.2×10^{-9}	7.2×10^{-8}
−0.50	3.3×10^{-10}	5.3×10^{-8}	8.8×10^{-8}	6.1×10^{-7}
0.00	5.0×10^{-9}	6.9×10^{-7}	7.1×10^{-7}	7.8×10^{-6}
0.50	4.6×10^{-10}	6.0×10^{-8}	5.3×10^{-8}	6.8×10^{-7}
1.00	6.4×10^{-10}	3.8×10^{-9}	6.3×10^{-9}	2.9×10^{-8}

Fig. 3. Comparison of proposed method solution by IADM and exact solution for −1 < x < 1 and (a) t = 0.1, (b) t = 0.2, (c) t = 0.3, (d) t = 0.5. (e) Profile of the solution q(x,t) and (f) density plot of the solution. Case m = 2 and subcase (iii) with N = 15.

Table 4
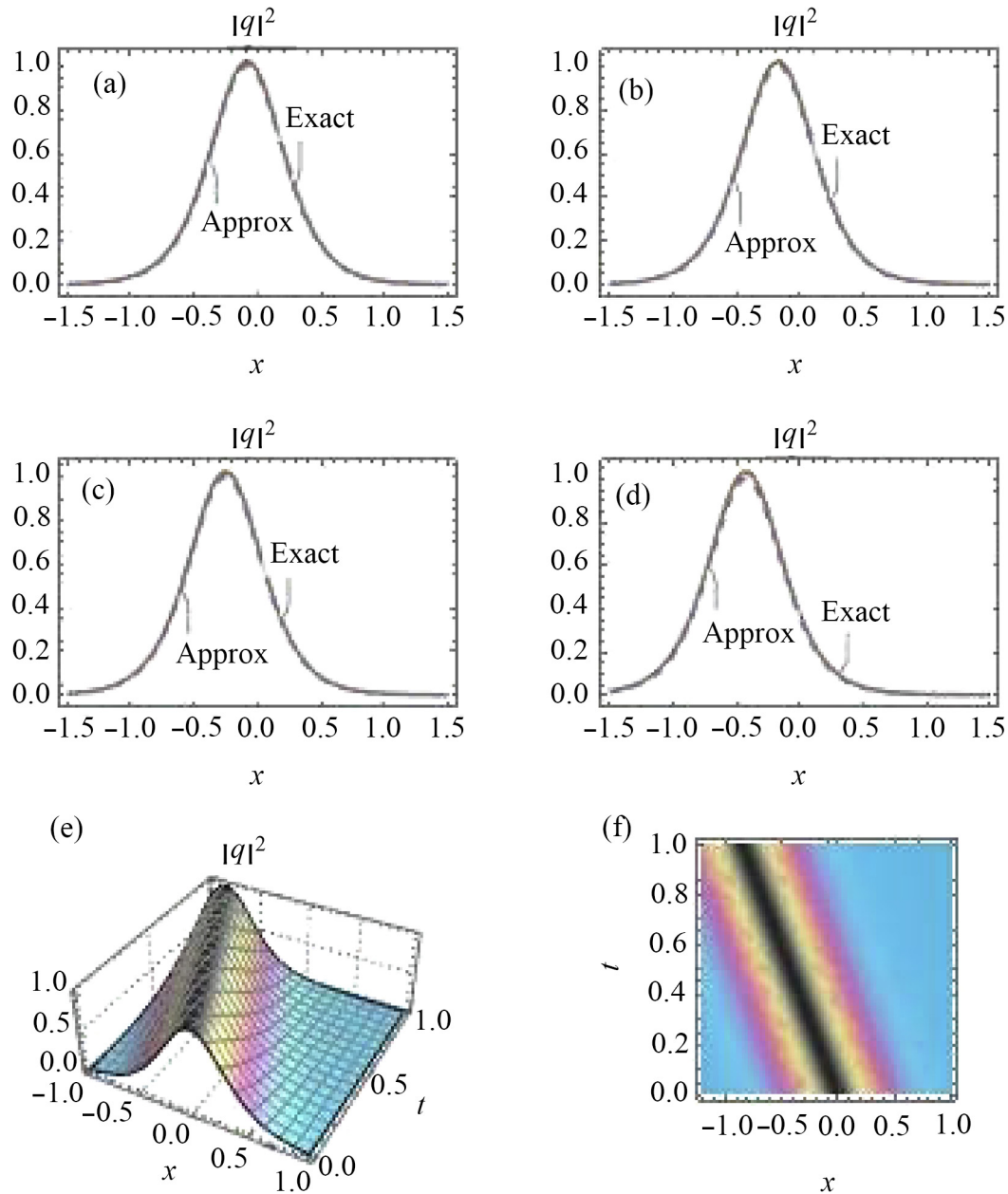The absolute error when t = 0.1, t = 0.2, t = 0.3 and t = 0.5 for case m = 2 and subcase (iv).

x	Error when t = 0.1	Error when t = 0.2	Error when t = 0.3	Error when t = 0.5
−1.50	8.9×10^{-10}	7.5×10^{-9}	5.1×10^{-9}	7.3×10^{-8}
−1.00	7.6×10^{-9}	7.4×10^{-9}	4.9×10^{-8}	6.7×10^{-7}
−0.50	1.2×10^{-9}	6.8×10^{-8}	8.3×10^{-7}	6.7×10^{-6}
0.00	2.9×10^{-8}	6.0×10^{-9}	5.6×10^{-7}	4.3×10^{-6}
0.50	1.0×10^{-9}	1.6×10^{-9}	7.2×10^{-8}	6.4×10^{-7}
1.00	2.9×10^{-9}	5.5×10^{-9}	8.7×10^{-9}	3.1×10^{-8}
1.50	4.0×10^{-10}	3.9×10^{-10}	6.4×10^{-9}	8.1×10^{-8}

Fig. 4. Comparison of proposed method solution by IADM and exact solution for $-1.5 < x < 1.5$ and (a) t = 0.1, (b) t = 0.2, (c) t = 0.3, (d) t = 0.5. (e) Profile of the solution q(x,t) and (f) density plot of the solution. Case m = 2 and subcase (iv) with N = 15.

$$\begin{cases} u_{2,0}(x,t) = g_0(x), \\ u_{2,k+1}(x,t) = g_{k+1}(x) + \int_0^t (-aR_3(u_{2,k}(x,\zeta) \\ +bR_4(u_{1,k}(x,\zeta)) + cA_{1,k})d\zeta, \ k \geqslant 0. \end{cases} \qquad (19)$$

From the above consideration, the solution will be approximated by two truncated series:

$$q(x,t) = u_1(x,t) + iu_2(x,t) \approx \sum_{n=0}^{N} u_{1,n}(x,t) + i\sum_{n=0}^{N} u_{2,n}(x,t). \qquad (20)$$

Results and discussion

In this section we give several examples to illustrate the efficiency and validity of the IADM and its application for the solution of the Eq. (1) in the case of bright solitons.

Case m = 1

Consider the CQ-NLSE model in Eq. (1) with the dispersion parameters and the power law of refractive index given in the following subcases:

(i) $a = \frac{1}{2}, b = -1$ and $c = 1$.
(ii) $a = \frac{1}{2}, b = -2$ and $c = -1$.

Case m = 2

Consider the CQ-NLSE model in Eq. (1) with the dispersion parameters and the power law of refractive index given in the following subcases:

(iii) $a = 1, b = -2$ and $c = 2$.
(iv) $a = 2, b = -1$ and $c = -3$.

To perform the simulations, we also consider the initial condition at $t = 0$ from Eq. (2)

$$q(x,0) = A\text{sech}^2[B(x)]e^{i[-\kappa x + \theta_0]}. \qquad (21)$$

Next we will present the simulation of the two cases (and the two subcases of each) above:

- In Table 1, we examine some values of t and compare with the results obtained from the exact solution for case $m = 1$ and subcase (i). For the same case and with the same parameters, the 2D simulations for values of from $t = 0.1, 0.2, 0.3, 0.5$ and 3D profile of the approximate solution and its respective density plot are shown in Fig. 1(a), (b), (c), (d), (e) and (f), respectively.
- In Table 2, we examine some values of t and compare with the results obtained from the exact solution for case $m = 1$ and subcase (ii). For the same case and with the same parameters, the 2D simulations for values of from $t = 0.1, 0.2, 0.3, 0.5$ and 3D profile of the approximate solution and its respective density plot are shown in Fig. 2(a), (b), (c), (d), (e) and (f), respectively.
- In Table 3, we examine some values of t and compare with the results obtained from the exact solution for case $m = 2$ and subcase (iii). For the same case and with the same parameters, the 2D simulations for values of from $t = 0.1, 0.2, 0.3, 0.5$ and 3D profile of the approximate solution and its respective density plot are shown in Fig. 3 (a), (b), (c), (d), (e) and (f), respectively.
- Finally, in Table 4, we examine some values of t and compare with the results obtained from the exact solution for case $m = 2$ and subcase (d). For the same case and with the same parameters, the 2D simulations for values of from

$t = 0.1, 0.2, 0.3, 0.5$ and 3D profile of the approximate solution and its respective density plot are shown in Fig. 4(a), (b), (c), (d), (e) and (f), respectively.

Conclusions

This paper discussed CQ solitons by the aid of IADM. The numerical results speak for itself with the display of impressive profiles for bright solitons. The results of the scheme thus pave way for future results. They will stem from CQ solitons from birefringent fibers having various nonlinear structures. Further along, the results will be extended to the model with DWDM networks. Those results will be available shortly down the road. Therefore those knowledge-hungry folks are suggested to hold it with patience!.

Declaration of Competing Interest

The authors declare they have no conflict of interest.

Compliance with Ethics Requirements

This article does not contain any studies with human or animal subjects.

Acknowledgments

References

[1] Anjan Biswas, Triki H, Zhou Q, Moshokoa SP, Ullah MZ, Belic M. Cubic-quartic optical solitons in Kerr and power law media. Optik 2017;144:357–62.
[2] Anjan Biswas, Ullah MZ, Zhou Q, Moshokoa SP, Triki H, Belic M. Resonant optical solitons with quadratic-cubic nonlinearity by semi-inverse variational principle. Optik 2017;145:18–21.
[3] Anjan Biswas, Kara AH, Ullah MZ, Zhou Q, Triki H, Belic M. Conservation laws for cubic-quartic optical solitons in Kerr and power law media. Optik 2017;145:650–4.
[4] Bansal A, Anjan Biswas, Zhou Q, Babatin MM. Lie symmetry analysis for cubic-quartic nonlinear Schrödinger's equation. Optik 2018;169:12–5.
[5] Anjan Biswas, Arshed S. Application of semi-inverse variational principle to cubic-quartic optical solitons with kerr and power law nonlinearity. Optik 2018;172:847–50.
[6] Das A, Anjan Biswas, Ekici M, Khan S, Zhou Q, Moshokoa SP. Suppressing internet bottleneck with fractional temporal evolution of cubic-quartic optical solitons. Optik 2019;182:303–7.
[7] Anjan Biswas, Ekici M, Sonmezoglu A, Belic MR. Highly dispersive optical solitons with quadratic-cubic law by exp-function. Optik 2019;186:431–5.
[8] Blanco-Redondo A, Sterke CMd, Sipe JE, Krauss TF, Eggleton BJ, Husko C. Pure-quartic solitons. Nat Commun 2016;7:10427.
[9] Abdel-Gawad HI, Osman M. On shallow water waves in a medium with time-dependent dispersion and nonlinearity coefficients. J Adv Res 2015;6:593–9.
[10] Yu W, Zhou Q, Mirzazadeh M, Liu W, Biswas Anjan. Phase shift, amplification, oscillation and attenuation of solitons in nonlinear optics. J Adv Res 2019;15:69–76.
[11] Wazwaz AM. A reliable modification of Adomian decomposition method. Appl Math Comput 1999;102:77–86.
[12] Wazwaz AM, El-Sayed SM. A new modification of the Adomian decomposition method for linear and nonlinear operators. Appl Math Comput 2001;122:393–405.
[13] Adomian G. Solving Frontier Problems of Physics: The Decomposition Method. Boston MA: Kluwer Academic Publishers; 1994.
[14] Kataria KK, Vellaisamy P. Simple parametrization methods for generating Adomian polynomials. Appl Anal Discr Math 2016;10:168–85.